J. Physiol. (1986), **376**, *pp.* 507–530
With 9 text-figures
Printed in Great Britain

INTRACELLULAR CALCIUM TRANSIENTS UNDERLYING THE SHORT-TERM FORCE–INTERVAL RELATIONSHIP IN FERRET VENTRICULAR MYOCARDIUM

BY W. GIL WIER AND DAVID T. YUE*

From the Department of Physiology, University of Maryland School of Medicine, 660 West Redwood Street, Baltimore, MD 21201, and the Department of Biomedical Engineering, The Johns Hopkins University School of Medicine, 720 Rutland Avenue, Baltimore, MD 21205 U.S.A.*

(*Received 16 July 1985*)

SUMMARY

1. The influence of short-term changes in stimulation pattern, both on the strength of contraction and on the amplitude of intracellular free-Ca^{2+} transients, was investigated in ferret papillary muscles. Intracellular free-Ca^{2+} concentration ($[Ca^{2+}]$) was assessed from the luminescence emitted from muscles microinjected with the Ca^{2+}-sensitive photoprotein aequorin.

2. The relationships between the strength of contraction and changes in stimulation pattern lasting 1–2 beats could be described by monoexponential functions, all with very similar time constants ($\sim$ 750 ms at 30 °C).

3. Over the entire range that could be obtained, the strength of contraction, quantified by either peak tension or peak rate of tension development, was found to be linearly correlated with peak estimated $[Ca^{2+}]$.

4. Potential errors in the estimation of $[Ca^{2+}]$ from aequorin luminescence were analysed. To assess the influence of spatial non-homogeneities of $[Ca^{2+}]$ on the estimate of $[Ca^{2+}]$, a model of Ca^{2+} diffusion in heart muscle was developed. The possible effect of using an inaccurate calibration curve was also examined. The results of these analyses indicate that $[Ca^{2+}]$ estimated from aequorin luminescence should be proportional to, if not equal to, true spatial average $[Ca^{2+}]$ (errors $< 7\%$).

5. Given the conclusion of the analysis described above, it is inferred from points 2 and 3 that the relationships between peak spatial average $[Ca^{2+}]$ and short-term changes in stimulation pattern are also represented by monoexponential functions, with time constants closely similar to those for the mechanical measurements.

6. Exposure to ryanodine, a substance believed to inhibit the release of Ca^{2+} from sarcoplasmic reticulum, produced striking alterations in the pattern of variations in $[Ca^{2+}]$ mentioned above. These alterations are consistent with the hypothesis that the functions described above depend essentially upon properties of the sarcoplasmic reticulum.

INTRODUCTION

Alterations in the strength of cardiac contraction produced by brief changes in stimulation pattern are described by the short-term force–interval relationship (Johnson, 1979). This relationship can be considered to derive from two properties: restitution (Braveny & Kruta, 1958) and post-extrasystolic potentiation (Hoffman, Bindler & Suckling, 1956). Restitution is exemplified by the recovery of contractile strength of an extrasystole observed when the interval between a steady-state and subsequent extrasystolic stimulus is lengthened. Post-extrasystolic potentiation is the enhancement of contractile strength of a post-extrasystole produced by shortening of the same interval. If these properties can be described quantitatively, then a general analytical expression can be written that predicts the strength of contraction following *any* 1–2 beat variation in stimulation pattern (eqn. (4) of Yue, Burkhoff, Franz, Hunter & Sagawa 1985*a*). In the mammalian left ventricle, a particularly simple expression was found: both restitution and potentiation were described by single exponential functions, all with the same time constant. This result led us (Burkhoff, Yue, Franz, Hunter & Sagawa, 1984; Yue *et al.* 1985*a*) to wonder whether restitution and potentiation might ultimately bear a direct and interpretable relation to properties of a single intracellular pool of Ca^{2+}.

In relation to this finding in the intact ventricle, the following three questions are raised in the present study. (i) Does cardiac muscle itself demonstrate the same phenomenon? (ii) If so, then to what extent might monoexponential functions describing the strength of contraction in muscle derive from similar functions governing the availability of activator Ca^{2+}? (iii) Is the sarcoplasmic reticulum (s.r.) required for the physiological expression of the functions for activator Ca^{2+}?

Our approach to these questions was to characterize, in ferret papillary muscles, the variations in force production and intracellular $[Ca^{2+}]$ produced by short-term changes in stimulation pattern. Intracellular free Ca^{2+} concentration ($[Ca^{2+}]$) was estimated from the luminescence emitted by muscles that had been microinjected with the bioluminescent protein aequorin. To aid in the quantitative interpretation of the intracellular Ca^{2+} transients, we developed a Ca^{2+} diffusion model for heart muscle. Finally, to evaluate the role of the s.r. in determining the observed pattern of variations in $[Ca^{2+}]$, we examined the effects of ryanodine, a plant alkaloid believed to block specifically the release of Ca^{2+} from s.r. (Sutko & Kenyon, 1983), upon these phenomena.

The results indicate that monoexponential functions, all with essentially the same time constant, characterize the restitution and potentiation of $[Ca^{2+}]$ as well as tension in isolated ventricular muscle. The s.r. appears to be essential to the physiological expression of these functions.

METHODS

Experimental arrangement

Hearts were excised from 8–12 week old ferrets (*Mustela putorius furo*) that had been anaesthetized with sodium pentobarbitone (80 mg kg^{-1}, I.P.). Papillary muscles $0{\cdot}67 \pm 0{\cdot}05$ mm (mean ± S.E of mean; $n = 7$) in external diameter were rapidly dissected from the right ventricle and placed in a continuously perfused bath chamber. The septal end of the muscle was held fixed in a clamp,

and the tendinous end was attached to a force transducer (Kulite Semiconductor Products, model BG-10). The superfusion solution contained (mM): NaCl, 92; $MgCl_2$, 1; KCl, 5; $NaHCO_3$, 20; Na_2HPO_4, 1; Na acetate, 20; glucose, 10; $CaCl_2$, 0·5–1·0. The solution was equilibrated with 95% O_2, 5% CO_2, resulting in pH 7·35. Perfusate temperature was kept constant at 30 °C by a Peltier device (Cambridge Thermionic Corp.) located beneath the bath. Muscles were stimulated at 0·2–0·5 Hz during a 1 h recovery period, after which 40–200 superficial cells were pressure-injected with aequorin (purchased from J. R. Blinks, Rochester, MN, U.S.A.) as described previously (Allen & Kurihara, 1980; Wier, 1980). Muscle length was then adjusted to produce maximum developed tension, and an opaque box was lowered over the bath to shield the preparation from external light during the experiments.

Measurements

Luminescence from the preparation was conducted to a photomultiplier tube (EMI 9893 B/350) by a Lucite light guide (6 mm diameter) located beneath the preparation. A parabolic mirror was positioned above the muscle. Photons were counted using an amplifier/discriminator (Princeton Applied Research, model 1121A), stored in digital form as counts per second, and signal averaged (Princeton Applied Research, model 4203) when required to improve the signal-to-noise ratio. Force signals were recorded simultaneously on magnetic tape (Hewlett–Packard, model 3964), and later converted to digital form.

Estimation of $[Ca^{2+}]$

The method of estimating $[Ca^{2+}]$ is analogous to that discussed previously (Allen & Blinks, 1978; Wier & Hess, 1984). Briefly, luminescence signals, L (in counts per second), were normalized by the maximal rate of light emission, L_{max} (determined as described below). The normalized light signal, termed the fractional luminescence (L/L_{max}), could then be used to obtain an estimate of $[Ca^{2+}]$ by referring to a calibration curve obtained *in vitro* (154 mM-KCl, 2 mM-$MgCl_2$, 5 mM-PIPES, pH 7·2, 30 °C) by the method of Blinks, Mattingly, Jewell, van Leeuwen, Harrer & Allen (1978) and described by:

$$L/L_{max} = \left\{\frac{1+K_R[Ca^{2+}]}{1+K_{TR}+K_R[Ca^{2+}]}\right\}^3, \quad (1)$$

where K_R represents the equilibrium constant for Ca^{2+} binding to the R state of aequorin, and K_{TR} represents the equilibrium constant of the transition between T and R states of aequorin. Under these conditions, $K_R = 4{\cdot}131 \times 10^{-6}$ M^{-1} and $K_{TR} = 151{\cdot}7$.

L_{max} was derived from the integral of light emitted when the preparation was lysed at the end of the experiment with 4% Triton X-100 and exposed to saturating $[Ca^{2+}]$. Before normalizing a particular signal L, however, the L_{max} estimated at the end of the experiment was adjusted for aequorin consumption ($\sim$ 10% for an entire experiment) by taking into account the integral of all the light emitted from the time at which a particular signal L was recorded to the end of the experiment (Wier, Kort, Stern, Lakatta & Marban, 1983).

Filtering of luminescence signals

To facilitate measurement of the peaks of $[Ca^{2+}]$ transients, L/L_{max} signals were digitally filtered by a low-pass window filter before measurement and display. The impulse response of the filter (symmetric FIR filter) was:

$$h(0) = 2f_c/f_s$$

$$h(\pm k) = \frac{\sin(2\pi k f_c/f_s)}{\pi k}(0{\cdot}54 + 0{\cdot}46\cos(\pi k/M)),$$

where $2M+1$ sampled points were used to derive a single filtered point, f_c was the cut-off frequency (= 25 Hz, −6 dB), and f_s was the sampling frequency (220–1000 Hz) (Ziemer, Tranter & Fannin, 1983). f_c was such that filtering did not distort significantly the L/L_{max} signals.

Stimulation protocols

A digital computer (IBM PC) interfaced to a timer-counter board (Tekmar, 'Labmaster' board) controlled a stimulus isolator (WPI, model PC-1) which supplied current to the muscle bath. The computer was programmed to produce the stimulation pattern illustrated by the schematized stimulation spikes at the top of Fig. 1.

During the 'priming period', muscles were stimulated by a series of 12–20 regularly timed stimuli delivered at a selected steady-state interval (s.s.i.) of between 1500 and 2000 ms. The priming period was long enough so that mechanical and luminescent responses to stimulation reached a steady state by the end of the period. An extrasystolic stimulus (giving rise to an extrasystole as labelled) followed the last regularly timed stimulus of the priming period by an interval called the extrasystolic interval(s) (e.s.i.). A post-extrasystolic stimulus (giving rise to a post-extrasystole as labelled) was then delivered which followed the extrasystolic stimulus by an interval called the post-extrasystolic interval(s) (p.e.s.i.). The p.e.s.i. was held fixed at 3000 ms. This sequence was repeated, and the steady state, extrasystolic and post-extrasystolic responses were averaged until an adequate signal-to-noise ratio was obtained for the luminescence signal (typically 16–32 sweeps). The e.s.i. was then changed, and the entire procedure repeated. The e.s.i. was varied from a value that elicited an extrasystolic contraction shortly after complete relaxation of tension of the steady-state beat up to at least 3000 ms.

Monoexponential curve-fitting procedure

Monoexponential functions were fitted to two types of curves (restitution curves and p.e.s.p. curves) to be described in the Results. The Taylor series method of non-linear least-squared error estimation (Draper & Smith, 1981) was used. The quality of the fit was estimated by the root mean squared error, normalized by the magnitude of the exponential, and expressed as percentage. 95% confidence intervals were determined for the time constants associated with the fitted monoexponential functions by using a linearized estimate of the variance–covariance matrix (Draper & Smith, 1981). Differences between two time constants were considered statistically significant when their 95% confidence intervals did not overlap.

RESULTS

Restitution and post-extrasystolic potentiation of the strength of contraction in muscle

Restitution and post-extrasystolic potentiation are illustrated by the original records of developed tension (F), derivative of tension (dF/dt), and [Ca^{2+}]-mediated luminescence (L/L_{max}) shown in Fig. 1. The records show steady-state, extrasystolic and post-extrasystolic responses stimulated according to the paradigm at the top of the Figure with e.s.i. ranging from 450 to 3000 ms. The traces have been aligned in time to superimpose steady-state responses. Restitution is exemplified by the monotonic recovery of F, dF/dt, and L/L_{max} of extrasystoles with lengthening e.s.i. Post-extrasystolic potentiation is demonstrated by the *decline* of F, dF/dt, and L/L_{max} of post-extrasystoles with lengthening of the e.s.i. Thus, the weakest extrasystole (a) precedes the strongest post-extrasystole (a'), and the strongest extrasystole (b) precedes the weakest post-extrasystole (b'). Increasing the e.s.i. beyond 3000 ms (up to 10000 ms, records not shown) produced no appreciable change in the strength of extrasystoles or post-extrasystoles from that manifested by the contractions labelled b and b', respectively. Hence, over the time scale considered in this study, the strength of both extrasystoles and post-extrasystoles was considered to reach a definite *plateau* as the e.s.i. was lengthened.

These records demonstrate two major points. First, the restitution and potentiation of the strength of contraction correspond closely to the restitution and potentiation of [Ca^{2+}]-mediated luminescence (L/L_{max}). We will consider this correspondence in detail in the next section of the Results. Secondly, as will be shown by the analysis to follow, the dependence of the strength of extrasystoles and post-extrasystoles upon the e.s.i. can be described by monoexponential functions.

The time course of the recovery of extrasystolic contractile strength was represented by restitution curves. Such curves were constructed by plotting peak developed F

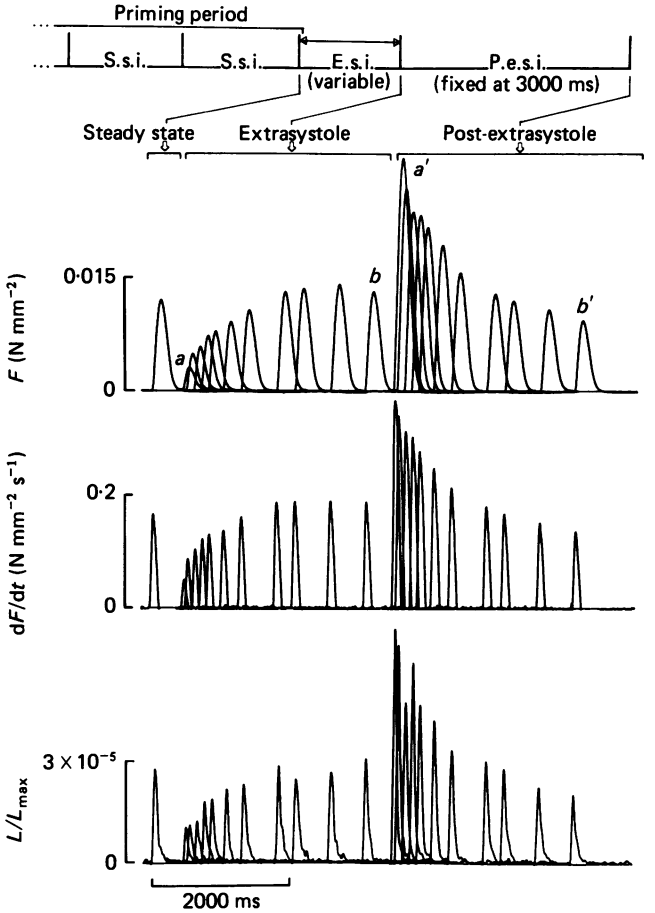

Fig. 1. Original records illustrating restitution and post-extrasystolic potentiation. The stimulation protocol that was used to produce the records is illustrated at the top. Traces show tension (top), rate of tension development (middle), and aequorin luminescence (bottom) from steady-state, extrasystolic, and post-extrasystolic beats. Records have been aligned in time to superimpose steady-state responses. Responses *a* and *a'* are from an extrasystole and subsequent post-extrasystole obtained with e.s.i. = 450 ms; *b* and *b'* correspond to e.s.i. = 3000 ms. S.s.i. was 1500 ms, and $[Ca^{2+}]_o$ = 0·7 mM. Traces are averages of sixteen to thirty-two sweeps.

(F_{max}) or peak dF/dt (dF/dt_{max}) as a function of the e.s.i. (Figs. 2*A* and *B*, respectively; derived from data in Fig. 1). F_{max} and dF/dt_{max} have been normalized by their respective steady-state values.

The decline of the strength of post-extrasystolic contraction with lengthening e.s.i. was graphically represented by post-extrasystolic potentiation (p.e.s.p.) curves, constructed by plotting F_{max} or dF/dt_{max} of post-extrasystoles (following a long p.e.s.i. equal to 3000 ms) as a function of the e.s.i. (Figs. 2*C* and *D*, respectively; derived from data in Fig. 1). F_{max} and dF/dt_{max} have been normalized by their respective steady-state values. Note, with reference to the restitution curves in Fig. 2*A* and *B*, that these post-extrasystoles are themselves fully restituted; in other

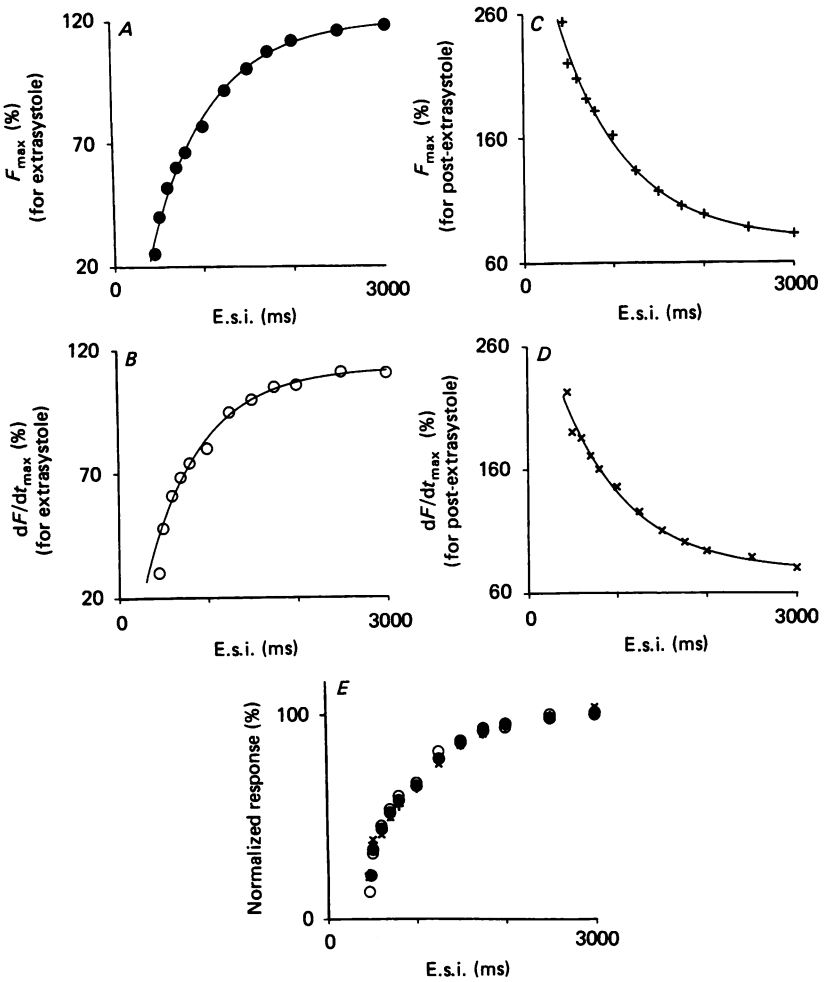

Fig. 2. Restitution (*A* and *B*) and post-extrasystolic potentiation (*C* and *D*) curves for peak tension (F_{max}) and peak rate of tension development (dF/dt_{max}). All responses have been normalized by their respective steady-state values and expressed as %. The continuous curves are least-squared error fits of monoexponential functions to the data. *E* shows that all four curves (*A–D*) superimpose after ordinate offsetting, amplitude scaling and inversion. This demonstrates that time constants for all curves are very similar. All curves derived from the data in Fig. 1.

words, for a given e.s.i., lengthening the p.e.s.i. beyond 3000 ms did not increase significantly the strength of post-extrasystoles.

Monoexponential functions were fitted to the restitution and p.e.s.p. curves in Fig. 2*A–D* (continuous curves) by a non-linear least-squared error algorithm. The time constants for the curves were quite similar: for F_{max}, 667 ms (*A*) and 747 ms (*C*); and for dF/dt_{max}, 626 ms (*B*) and 753 ms (*D*). There was no statistical significance among these values ($P > 0{\cdot}05$). This is demonstrated intuitively in Fig. 2*E* where the restitution and p.e.s.p. curves from Fig. 2*A–D* all superimpose after ordinate offsetting, scaling in amplitude, and inverting in the case of p.e.s.p. curves. These results were confirmed in a total six muscles (Table 1).

TABLE 1. Summary of exponential regression of restitution curves (r.c.) and p.e.s.p. curves (p.e.s.p.c.)

Time constants (ms)

F_{max}		dF/dt_{max}	
R.c.	P.e.s.p.c.	R.c.	P.e.s.p.c.
765±48	864±66	708±60	814±37

The Table is derived from eight sets of curves (r.c. and p.e.s.p.c. determined with F_{max} and dF/dt_{max}), measured in six muscles. The results are expressed as the mean±S.E. of mean. In six of eight sets of curves there was no statistical significance ($P > 0.05$) to the differences between time constants for any of the four types of curves specified above. The root-mean-squared normalized error for the thirty-two curves measured was 2·81±0·25% (mean±S.E. of mean), indicating that the curves were well fitted by the monoexponential form.

Thus, the functions describing the restitution and post-extrasystolic potentiation of the strength of contraction in muscle are well approximated by monoexponential functions with essentially the same time constant, suggesting that the very similar results observed previously in the intact ventricle (Yue *et al.* 1985*a*) are attributable to intrinsic muscle properties.

The results shown in Fig. 1 were typical for ferret papillary muscles exposed to extracellular $[Ca^{2+}]$ ($[Ca^{2+}]_o$) of 0·5–1·0 mM. Whereas exposure to higher $[Ca^{2+}]_o$ did not affect restitution significantly, it did reduce (but never abolished) the potentiation of post-extrasystoles produced by shortening e.s.i. A low $[Ca^{2+}]_o$ was used because this enabled a range of post-extrasystolic potentiation similar to that observed in the blood-perfused canine ventricle at 37 °C (Yue *et al.* 1985*a*). Force measurements in rabbit papillary muscles yielded results similar to those in Figs. 1 and 2, even at higher $[Ca^{2+}]_o$ (up to 3·5 mM) (D. T. Yue, unpublished observations).

Relationship of changes in the strength of contraction to variations in free $[Ca^{2+}]$

From Fig. 1, it is apparent that the restitution and potentiation of the strength of contraction parallel changes in $[Ca^{2+}]$, but how close is this correlation quantitatively? To examine this question, we consider the relationship between F_{max}, dF/dt_{max} and peak $[Ca^{2+}]$ (taken here to be synonymous with the availability of activator Ca^{2+}).

Fig. 3*A* and *B* shows plots of F_{max} *vs.* peak L/L_{max}, and of dF/dt_{max} *vs.* peak L/L_{max}, respectively, derived from steady-state beats, extrasystoles and post-extrasystoles used to determine the restitution and p.e.s.p. curves. These relationships are curvilinear. After converting L/L_{max} to estimated $[Ca^{2+}]$, however, we find that the relationships of F_{max} *vs.* peak $[Ca^{2+}]$, and of dF/dt_{max} *vs.* peak $[Ca^{2+}]$, are quite linear (Fig. 3*C* and *D*). Linear regression provides excellent fits to the data as shown (for F_{max}, slope = 0·0396 N mm^{-2} μM^{-1}, $[Ca^{2+}]$-axis intercept = 0·42 μM, $r = 0.97$; and for dF/dt_{max}, slope = 0·433 N mm^{-2} s^{-1} μM^{-1}, $[Ca^{2+}]$-axis intercept = 0·31 μM, $r = 0.97$). These results were found in a total of five muscles (Table 2). Similar results have been found in canine Purkinje fibres (Yue, Wier & Sagawa, 1984).

We caution that the uncertainty in our estimate of $[Ca^{2+}]$ from aequorin luminescence may be considerable; the potential sources of error and their likely implica-

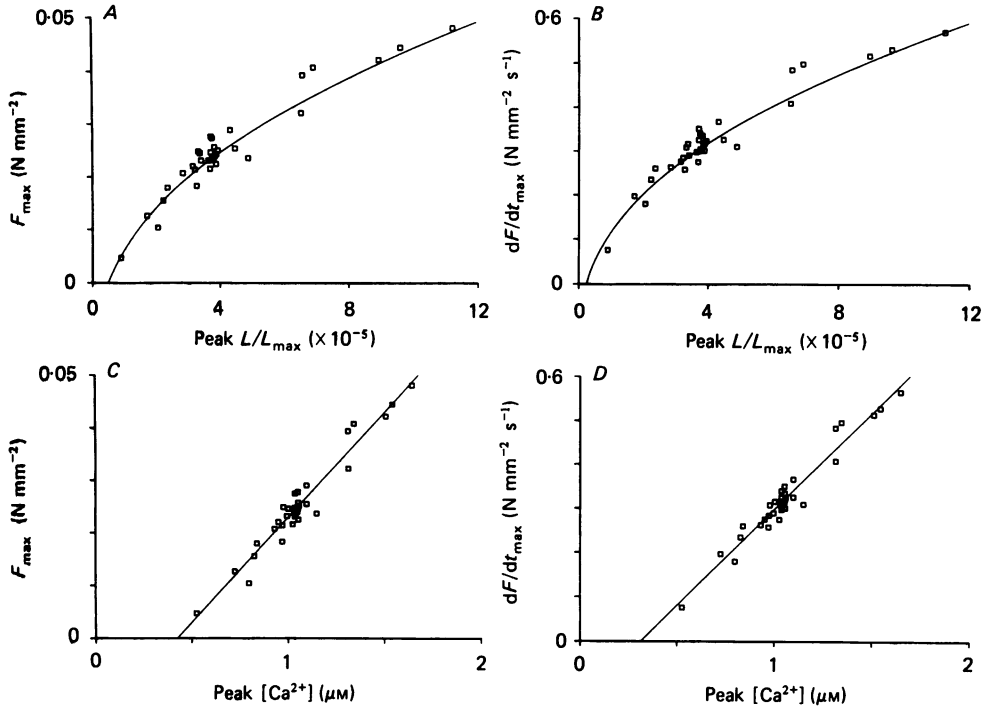

Fig. 3. Relation of peak aequorin luminescence (L/L_{max}) to F_{max} (A), and to dF/dt_{max} (B) derived from variably restituted and potentiated beats. The continuous curves in A and B are of the form F_{max} or $dF/dt_{max} = G \times (L/L_{max})^{1/2.37} + H$ ($G = 2.965$ N mm^{-2} and $H = 0.017$ N mm^{-2} in A; $G = 32.418$ N mm^{-2} s^{-1} and $H = 0.134$ N mm^{-2} s^{-1} in B). C and D show the same relations after peak L/L_{max} has been calibrated to peak [Ca^{2+}]. The continuous lines in C and D were fitted to the data by linear regression.

TABLE 2. Summary of relationships between F_{max}, dF/dt_{max}, estimated peak intracellular [Ca^{2+}] and L/L_{max}

	F_{max} *vs.* peak [Ca^{2+}]	dF/dt_{max} *vs.* peak [Ca^{2+}]
Slope	0·03 ± 0·0024 N mm^{-2} μM^{-1}	0·337 ± 0·0238 N mm^{-2} s^{-1} μM^{-1}
[Ca^{2+}]-axis intercept	0·51 ± 0·07 μM	0·38 ± 0·07 μM
Correlation coefficient (r)	0·96 ± 0·01	0·96 ± 0·01
	F_{max} *vs.* peak L/L_{max}	dF/dt *vs.* peak L/L_{max}
G	2·245 ± 0·181 N mm^{-2}	25·242 ± 1·783 N mm^{-2} s^{-1}
H	0·015 ± 0·002 N mm^{-2}	0·129 ± 0·025 N mm^{-2} s^{-1}

Results were obtained from five muscles, and expressed as the mean ± S.E. of mean.

tions for the interpretation of these results will be evaluated in the Discussion. For the moment, suffice it to say that the strength of contraction relates quite linearly to peak *estimated* [Ca^{2+}]. Thus, to the extent that estimated [Ca^{2+}] is correct, this linearity implies that the restitution and potentiation of peak [Ca^{2+}] should also be described by monoexponential functions, with time constant identical to that determined from mechanical measurements. However, the non-zero [Ca^{2+}]-axis intercept values (Fig. 3C and D and Table 2) imply that the amplitude and plateau values of the

monoexponential functions describing the restitution and potentiation of peak $[Ca^{2+}]$ would differ from those functions determined from F_{max} or dF/dt_{max}.

These conclusions were consistent with results obtained by fitting monoexponential functions to restitution and p.e.s.p. curves derived from peak $[Ca^{2+}]$. The time constants derived for such curves were not statistically distinguishable from those determined for F_{max} or dF/dt_{max} in any of the preparations. However, because of the sensitivity of non-linear regression analysis to noise, statistical fluctuations of luminescence (along with minor drifts in the estimate of $[Ca^{2+}]$ for steady-state responses) resulted in confidence intervals for time constants derived from peak $[Ca^{2+}]$ that were too wide to be conclusive (typically ± 500 ms, compared to ± 100 ms for mechanical responses). The linear regression analysis presented above was therefore felt to be the more reliable method for assessing the nature of the restitution and p.e.s.p. curves for peak $[Ca^{2+}]$.

Since the relation between the strength of contraction and peak estimated $[Ca^{2+}]$ is linear, and the aequorin calibration curve is well approximated over the working range (0–2 μM) by

$$L/L_{max} = 3{\cdot}61 \times 10^{-5} \times \{[Ca^{2+}]\,(\mu M)\}^{2{\cdot}37},$$

a simple analytical characterization of the relationship between F_{max} and L/L_{max}, and between dF/dt_{max} and L/L_{max}, is easily determined from the linear regression analysis:

$$F_{max} \quad \text{or} \quad dF/dt_{max} = G \times (L/L_{max})^{1/2{\cdot}37} + H,$$

where G and H are constants. The continuous curves show the fit of this expression to the data in Fig. 3*A* and *B*. Mean values for G and H from five muscles are tabulated in Table 2.

Effect of ryanodine upon restitution and post-extrasystolic potentiation

If the same time constant characterizes both the restitution and the post-extrasystolic potentiation of peak free $[Ca^{2+}]$, a single cellular process, perhaps Ca^{2+} uptake and/or release of the s.r., may fundamentally underlie both of these phenomena. In accordance with this expectation, we found that ryanodine, a substance believed to inhibit specifically Ca^{2+} release from the s.r., has dramatic and interpretable effects upon *both* restitution and post-extrasystolic potentiation.

Fig. 4 shows records of F, dF/dt, and L/L_{max} from steady-state, extrasystolic and post-extrasystolic responses obtained during exposure to 5 μM-ryanodine. The stimulation pattern was the same as in Fig. 1. These records demonstrate two major effects of ryanodine.

First, a striking acceleration of the time course of restitution was produced. This is demonstrated most clearly by the original records of $[Ca^{2+}]$-regulated luminescence (L/L_{max}). In the record corresponding to e.s.i. = 340 ms, the extrasystolic stimulus fell just within the refractory period, so that no extrasystole was elicited. When the e.s.i. was increased to 375 ms, an extrasystolic L/L_{max} response, somewhat smaller than the steady-state response, was observed. If the e.s.i. was increased by only 25 ms, the extrasystolic response became virtually the same as the steady-state one (e.s.i. 400 ms). Further lengthening of the e.s.i. (800 and 3000 ms) produced very little

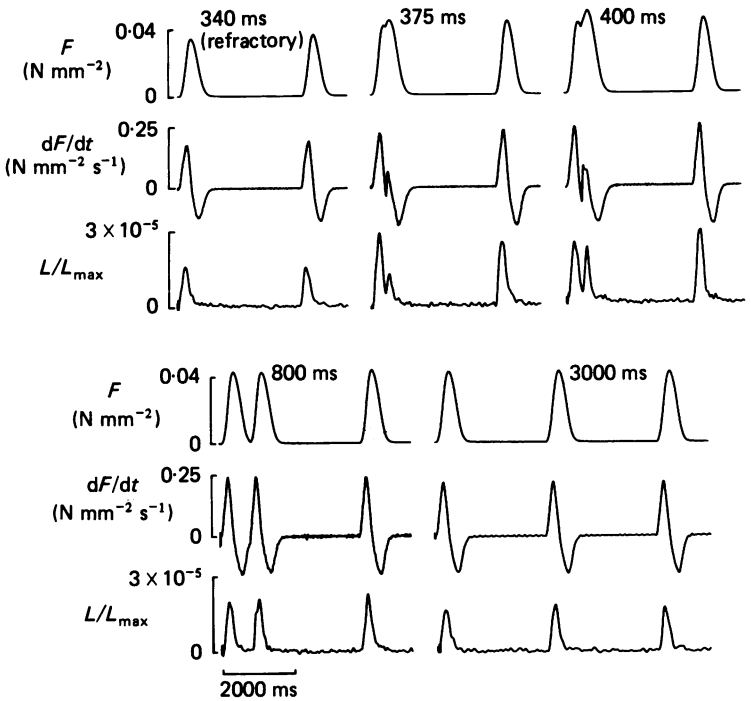

Fig. 4. Original records illustrating the effects of 5 μM-ryanodine on restitution and post-extrasystolic potentiation. The stimulation protocol was the same as that illustrated in Fig. 1, with s.s.i. = 1500 ms. Each frame corresponds to the indicated e.s.i., and contains records of tension (F), derivative of tension (dF/dt), and aequorin light (L/L_{max}) from steady-state, extrasystolic, and post-extrasystolic beats. The records indicate that restitution was greatly accelerated and post-extrasystolic potentiation was abolished. No extrasystole appears at e.s.i. = 340 ms because the muscle was just refractory. We note small drifts in the magnitude of steady-state responses among the protocols; the effect of these were minimized by the normalization procedure used to construct the restitution and p.e.s.p. curves in Fig. 5. To improve the signal-to-noise ratio of the luminescence signals obtained during exposure to ryanodine, data shown here were obtained in $[Ca^{2+}]_o$ = 3 mM instead of the $[Ca^{2+}]_o \sim 0{\cdot}7$ mM used to obtain physiological restitution and p.e.s.p. curves. It was confirmed that the use of a higher $[Ca^{2+}]_o$ did not itself produce the marked effects shown. Records are averages of fifty sweeps.

additional enhancement of extrasystolic responses. The detailed restitution curve for peak L/L_{max} (Fig. 5C, constructed exactly as described for the restitution curve of F_{max} or dF/dt_{max}) shows that the restitution of activator Ca^{2+} proceeded essentially to completion within the 100 ms following the refractory period. The arrow indicates the e.s.i. at which the muscle was just refractory. The original records of F and dF/dt (Fig. 4, e.s.i. 800 and 3000 ms), and the restitution curve of F_{max} and dF/dt_{max} (Fig. 5A and B) are consistent with these findings, although the interpretation of F_{max} and dF/dt_{max} for e.s.i. < 800 ms was uncertain because of fusion of extrasystolic and steady-state responses (e.g. Fig. 4, e.s.i. 375 and 400 ms).

The second effect of ryanodine was to abolish post-extrasystolic potentiation, consistent with the prior observation that ryanodine eliminates paired-pulse potentiation in cat papillary muscle (Sutko, Willerson, Templeton, Jones & Besch, 1979). Fig. 4 (e.s.i. 340 *vs.* 375 ms) demonstrates that the strength of a post-extrasystole

is independent of whether an extrasystole was present or not. Variations in e.s.i. (Fig. 4, 800 and 3000 ms) did not alter appreciably the strength of post-extrasystoles. In other words, post-extrasystolic responses were virtually independent of the e.s.i., as demonstrated by the flat p.e.s.p. curve for F_{max}, dF/dt_{max} and peak L/L_{max} (Fig. 5*D–F*). The p.e.s.p. curve for L/L_{max} was constructed exactly as for F_{max} or dF/dt_{max}.

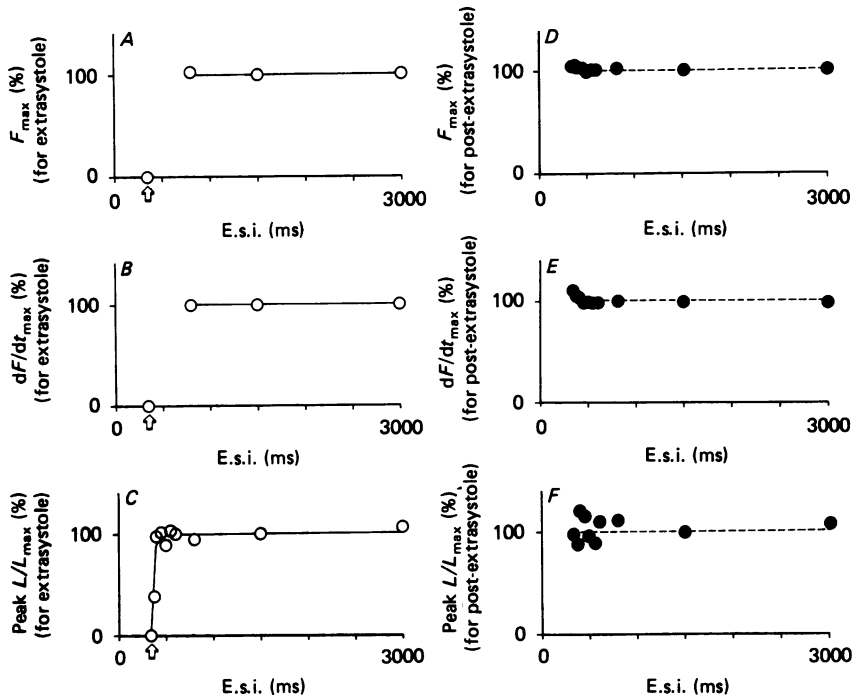

Fig. 5. Restitution (*A*, *B* and *C*) and p.e.s.p. (*D*, *E* and *F*) curves for F_{max}, dF/dt_{max}, and peak L/L_{max}, obtained during exposure to 5 μM-ryanodine. All responses were normalized by their respective steady-state values. The arrows in panels *A–C* indicate the e.s.i. at which the muscle was just refractory. The portions of the restitution curves for F_{max} (*A*) and dF/dt_{max} (*B*) corresponding to e.s.i. = 340–800 ms were not plotted because steady-state and extrasystolic tension responses were 'fused' together. All curves derived from same preparation as in Fig. 4.

Because both the restitution and p.e.s.p. curves were markedly affected by ryanodine, the findings suggest that intact s.r. function is essential for both the restitution and the post-extrasystolic potentiation of $[Ca^{2+}]$ observed under physiological conditions. A more detailed interpretation of the effects of ryanodine described above will be presented in the Discussion.

DISCUSSION

We focus here on three aspects of the results: (a) an evaluation of the potential limitations of our estimate of $[Ca^{2+}]$, (b) the implications of these upon the interpretation of the linear relation between the strength of contraction and peak

estimated [Ca^{2+}] and (c) the interpretation of the restitution and post-extrasystolic potentiation of peak [Ca^{2+}] before and during exposure to ryanodine.

Potential limitations of the determination of intracellular [Ca^{2+}]

I. Effects of spatial non-homogeneities of [Ca^{2+}] *upon the estimate of* [Ca^{2+}] *from aequorin luminescence*

The upward convexity of the aequorin calibration curve ($d^2(L/L_{max})/d([Ca^{2+}])^2 > 0$) contributes a major uncertainty to the estimate of [Ca^{2+}] from aequorin luminescence collected from an entire preparation. Because of the convexity, the estimate of [Ca^{2+}] will be greater than spatial average [Ca^{2+}] whenever spatial non-homogeneities of [Ca^{2+}] are present (Baker, Hodgkin & Ridgway, 1971; Yue & Wier, 1985). To assess the extent of the over-estimate, we developed the following model of Ca^{2+} diffusion in heart muscle. The model is an adaptation of the skeletal muscle diffusion model reported previously by Cannell & Allen (1984).

(*a*) *Description of model*

(*i*) *Appropriate physical scale for the model.* We assume that the appropriate scale over which to consider diffusion is the half-sarcomere because most of the Ca^{2+} supplied to the myoplasm is believed to be derived from the s.r. (e.g. estimates of $\sim 100\%$ (Fabiato, 1983; Marban & Wier, 1985); there is further discourse about this point at the end of the Discussion), and the s.r. is evenly distributed about each half-sarcomere (Sommer & Johnson, 1979). Moreover, branches of an extensive T-tubular network closely appose the s.r., especially near the z-line of almost every sarcomere (Sommer & Johnson, 1979), providing a means to synchronize Ca^{2+} release throughout the muscle. Finally, for the majority of sarcomeres located inward from the periphery of the cardiac cell, trans-sarcolemmal Ca^{2+} fluxes would be seen to occur primarily through the T-tubules surrounding the z-line. Thus, cardiac muscle seems to be composed of a multiplicity of synchronized half-sarcomeres; we only need consider one.

(*ii*) *Physical characteristics of the model.* As shown in Fig. 6, the half-sarcomere is assumed to be cylindrical, with a radius (R) of 0·5 μm, and length (SL) of 1·0 μm (Sommer & Johnson, 1979). The s.r. network was approximated by a continuous sheath surrounding the myofibrillar space (m.f.s.); the lateral one-fifth of the sheath (near the z-line) was considered junctional s.r. (j.s.r.), while the remainder of the sheath was considered free s.r. (f.s.r.). The m.f.s. was assumed to be uniformly populated with non-diffusible Ca^{2+}-specific binding sites of troponin (TR) and calmodulin (CM). These are the only Ca^{2+} buffers expected to have sufficiently fast kinetics to respond significantly to physiological [Ca^{2+}] transients (Robertson, Johnson & Potter, 1981).

(*iii*) *Ca^{2+} fluxes.* To obtain an upper limit estimate of the magnitude of the spatial gradients of [Ca^{2+}] that could exist in cardiac muscle, we have assumed that Ca^{2+} release occurs only from j.s.r. (Fig. 6, CR), and that Ca^{2+} sequestration (Fig. 6, CS) occurs only in f.s.r. Had we assumed that release and sequestration of Ca^{2+} occurred in both j.s.r. and f.s.r., longitudinal gradients of [Ca^{2+}] would have become negligible. The surface flux of Ca^{2+} release from j.s.r. into the m.f.s. was assumed to be of the form:

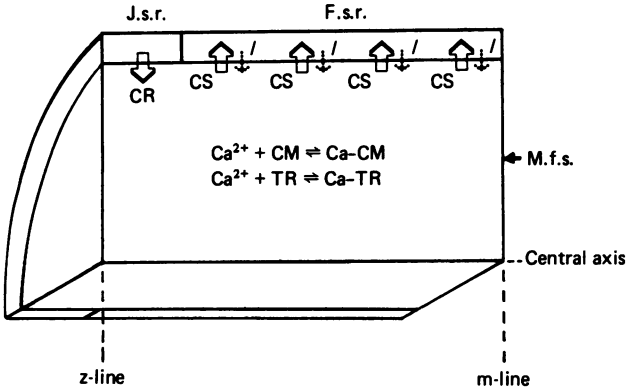

Fig. 6. Physical characteristics of the model of Ca^{2+} diffusion. A 'wedge' from a half-sarcomere is shown. The junctional s.r. (j.s.r.) releases Ca^{2+} (CR) into the myofibrillar space (m.f.s.). Ca^{2+} can diffuse, bind to calmodulin (CM) or troponin (TR), or be sequestered (CS) by free s.r. (f.s.r.). A leakage flux of Ca^{2+} (l) is assumed from f.s.r. to maintain resting $[Ca^{2+}] = 0{\cdot}1$ μM in the absence of Ca^{2+} release.

$$\mathrm{CR} = \frac{R_{\max}}{2}\left[1 - \cos\frac{(2\pi t)}{0{\cdot}05}\right] \quad \text{for} \quad t\colon 0 < t < 0{\cdot}05 \text{ s}, \tag{2}$$

$$\mathrm{CR} = 0 \quad \text{for} \quad t\colon 0{\cdot}05 \text{ s} < t,$$

where $R_{\max}$, the maximum surface flux, was adjusted to 3·00 μmol s^{-1} m^{-2} to yield a realistic intracellular $[Ca^{2+}]$ transient amplitude, and the surface area at the j.s.r.–m.f.s. interface is $6{\cdot}283 \times 10^{-13}$ m^2. Ca^{2+} in the m.f.s. can diffuse according to the free diffusion coefficient (D) of 7×10^{-10} m^2 s^{-1} (Wang, 1953), react with binding sites on troponin or calmodulin, or be taken up by f.s.r. Since Ca^{2+} entry across the T-tubules would occur near the j.s.r.–m.f.s. interface, the influx of Ca^{2+} was considered to be lumped in with the release of Ca^{2+} from j.s.r. (Fig. 6, CR). Ca^{2+} efflux across the T-tubules would also arise from near the j.s.r., and would therefore be geometrically equivalent to allowing the j.s.r. to sequester Ca^{2+}. Since this would reduce the magnitude of spatial gradients of $[Ca^{2+}]$, we neglected this efflux process. A constant leakage flux of Ca^{2+} (Fig. 6, l) from f.s.r. is assumed so that resting $[Ca^{2+}]$ is 0·1 μM in the absence of Ca^{2+} release.

(*iv*) *Simulation of the estimate of* $[Ca^{2+}]$ *derived from aequorin luminescence.* Aequorin was assumed to be uniformly distributed throughout the myofibrillar compartment. The evidence favouring this assumption has been evaluated elsewhere (Blinks, Wier, Hess & Prendergast, 1982). The simulated fractional luminescence emitted from the entire half-sarcomere was therefore given by:

$$(1/V_{\mathrm{T}}) \iiint_P L/L_{\max}([Ca^{2+}])\,dx\,dy\,dz, \tag{3}$$

where the expression for $L/L_{\max}$ is given in eqn. (1), P is the volume region defined by the m.f.s., and V_{T} is the volume of region P. The simulated estimate of $[Ca^{2+}]$ derived from aequorin luminescence was obtained by referring the value given by eqn. (3) to the calibration curve (eqn. (1)). Delays in the response of aequorin to

changes in $[Ca^{2+}]$ were evaluated and determined to be negligible on the time scale of interest. In this evaluation, we assumed that aequorin luminescence responded to changes in $[Ca^{2+}]$ as a first-order low-pass filter with time constant $\sim$ 5 ms (Neering & Wier, 1980). Further details of the simulation are presented in the Appendix and Table 3.

TABLE 3. Summary of parameters of Ca^{2+} diffusion model

Parameter	Value	Source
Half-sarcomere dimensions	(*SL*) length 1×10^{-6} m	(Sommer & Johnson, 1979)
	(*R*) radius 5×10^{-7} m	(Sommer & Johnson, 1979)
Free diffusion coefficient (*D*)	7×10^{-10} mm^2 s^{-1}	(Wang, 1953)
Maximum surface flux of Ca^{2+} release from j.s.r. (R_{max})	3 μmol s^{-1} m^{-2}	(Present study)
Maximum surface flux of Ca^{2+} uptake into f.s.r. (V_{max})	0·223 μmol s^{-1} m^{-2}	(Present study)
$[Ca^{2+}]$ required for half-maximal Ca^{2+} uptake into f.s.r. (K_m)	0·25 μM	(Present study)
Surface leakage flux from f.s.r. (*l*)	$6{\cdot}377 \times 10^{-2}$ μmol s^{-1} m^{-2}	(Present study)
Ca^{2+}-specific troponin binding sites		
Concentration	70 μM	(Solaro *et al.* 1974)*
Ca^{2+} on rate	$3{\cdot}9 \times 10^7$ M^{-1} s^{-1}	(Robertson *et al.* 1981)
Ca^{2+} off rate	19·6 s^{-1}	(Robertson *et al.* 1981)
Calmodulin binding sites		
Concentration	50 μM	(Cheung, 1980)*
Ca on rate	$1 \times 10^{+8}$ M^{-1} s^{-1}	(Robertson *et al.* 1981)
Ca off rate	238 s^{-1}	(Robertson *et al.* 1981)

* Literature values in μmol kg^{-1} wet weight were divided by 0·4 to convert to μmol l^{-1} myoplasm exposed to free $[Ca^{2+}]$. The value of 0·4 was based upon: (a) tissue wet weight $\times$ 0·77 = water weight (Polimeni, 1974), (b) water weight $\times$ 0·75 = intracellular water weight (Polimeni, 1974), (c) 1 kg intracellular water weight $\sim$ litre of intracellular volume (Page, 1978), (d) mitochondrial volume = 0·36 $\times$ intracellular volume (Page, 1978), and (e) myoplasmic volume $\sim$ intracellular volume − mitochondrial volume = 0·64 $\times$ intracellular volume (from (d)). Thus, 0·4 $\sim$ 0·77 $\times$ 0·75 $\times$ 0·64.

(*b*) *Prediction of errors in the estimate of spatial average* $[Ca^{2+}]$ *derived from aequorin luminescence*

Fig. 7*A* demonstrates that the $[Ca^{2+}]$ transient measured experimentally for a phasic contraction (upper trace) is similar to that produced by the model (bottom trace). Both signals peak at $\sim$ 42 ms; the experimental signal declines to half its peak value by 73 ms into the transient, whereas the model signal declines slightly faster, reaching half its peak value by 60 ms.

The model also demonstrates that $[Ca^{2+}]$ is spatially non-homogeneous to a moderate degree during the release of Ca^{2+} (which occurs between 0 and 50 ms; eqn. (2)), but that $[Ca^{2+}]$ becomes spatially uniform by 5 ms after the release (13 ms after the peak of luminescence). This is illustrated by the plots of $[Ca^{2+}]$ as a function of radial and longitudinal coordinates (Fig. 7*B*). The bottom of each plot corresponds

to a slice through the half-sarcomere as illustrated by the drawing at the left of the plots. Spatial gradients of $[Ca^{2+}]$ increase initially (20 ms), become most severe just before the peak of the $[Ca^{2+}]$ transient (40 ms), but are negligible during the decline of the transient (70 ms). Fig. 7*C* provides a more detailed representation of the time course of the spatial gradients of $[Ca^{2+}]$. Spatial average $[Ca^{2+}]$ (continuous curve) with bracketing spatial standard deviations of $[Ca^{2+}]$ (dashed curves) are plotted as a function of time.

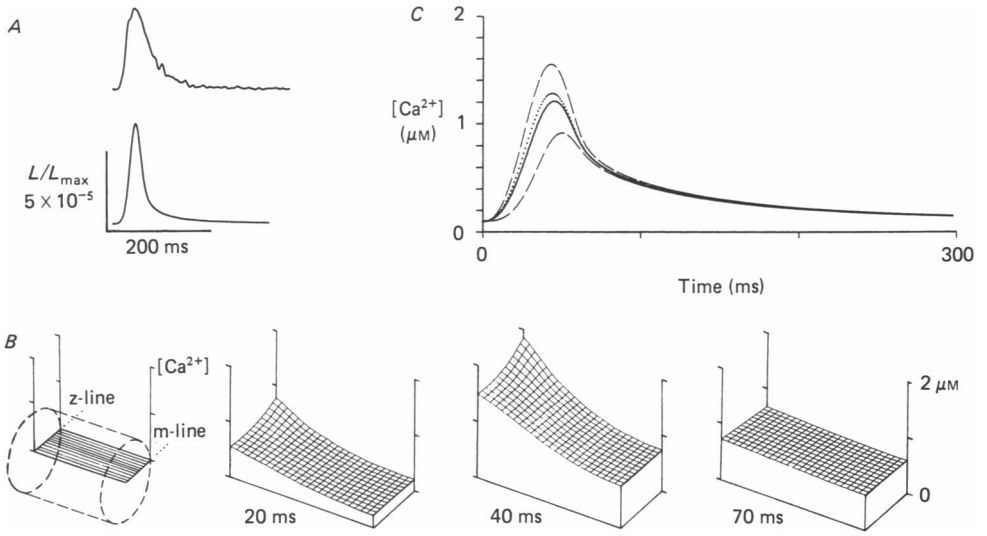

Fig. 7. Results of the model of Ca^{2+} diffusion in heart muscle. *A*, actual (top) and simulated (bottom) aequorin light. *B*, $[Ca^{2+}]$ plotted as a function of radial and longitudinal coordinates in the half-sarcomere. The plots correspond to three instances in the cardiac twitch as labelled. Relation of plots to the geometry of the half-sarcomere is illustrated at the far left. *C*, time plots of spatial average $[Ca^{2+}]$ (continuous curve), bracketing spatial standard deviations of $[Ca^{2+}]$ (dashed curves) and $[Ca^{2+}]$ estimated from aequorin luminescence (dotted curve).

A striking prediction of the model is that, despite the presence of moderately large spatial gradients of $[Ca^{2+}]$, the estimate of $[Ca^{2+}]$ derived from aequorin luminescence (Fig. 7*C*, dotted curve) is in excellent agreement with true spatial average intracellular $[Ca^{2+}]$ *throughout* the transient. In this particular run, the error in the estimate of spatial average $[Ca^{2+}]$ was no more than 7 %.

The sensitivity of the model predictions to wide variations in the maximum Ca^{2+} release flux (R_{max} in eqn. (2)), the maximum Ca^{2+} sequestration flux (V_{max} in eqn. (A 2) in the Appendix), and the $[Ca^{2+}]$ at which the s.r. pump rate was half-maximal (K_m in eqn. (A 2)) was investigated. We invariably found that: (1) the estimate of $[Ca^{2+}]$ derived from aequorin luminescence closely approximated true spatial average $[Ca^{2+}]$ (< 10 % error) and (2) $[Ca^{2+}]$ became spatially uniform within 15 ms following the peak of the $[Ca^{2+}]$ transient ($\sim$ the end of Ca^{2+} release).

II. Effect of the use of an inappropriate calibration curve on the estimate of $[Ca^{2+}]$ *from aequorin luminescence*

The other major concern regarding the estimate of $[Ca^{2+}]$ from aequorin luminescence is that the conditions under which the calibration curve was determined *in vitro* might not adequately mimic the intracellular milieu. The main uncertainty is the value of intracellular $[Mg^{2+}]$ which was assumed to apply *in vivo* ($\sim$ 2 mM, based on nuclear magnetic resonance studies of Cohen & Burt (1977) along with Dawson, Gadian & Wilkie (1978)).

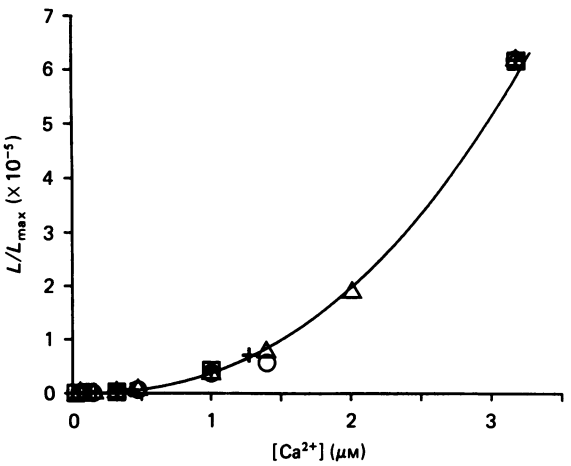

Fig. 8. Superposition of different aequorin calibration curves after normalization in amplitude. Curves have been scaled so that $L/L_{max} \sim 6{\cdot}1 \times 10^{-5}$ at 3·16 μM. The curves have been obtained under very different conditions. Those obtained at 20 °C in 0 (□), 3 (+) and 6 (○) mM-$MgCl_2$ (150 mM-KCl, 5 mM-PIPES, pH 7·0) are from Moore (1984). △ represents the curve used in this study (obtained at 30 °C in 2 mM-$MgCl_2$, 154 mM-KCl, 5 mM-PIPES, pH 7·2). The continuous curve is eqn. (4) with $A = 3{\cdot}79 \times 10^{-5}$.

A little-noted phenomenon, however, is that, over the important range of the calibration curve ($[Ca^{2+}] = 0$–3 μM), the effect of variations in $[Mg^{2+}]$, temperature and perhaps other conditions can be represented approximately by a simple change in the amplitude of the curve. This phenomenon is demonstrated by the superposition of calibration curves obtained under very different conditions, after normalization of the curves in amplitude (Fig. 8). All of these curves can be approximated by:

$$L/L_{max} = A \times \{[Ca^{2+}]\,(\mu M)\}^{2{\cdot}37}, \quad (4)$$

where A is a constant particular to a given set of conditions (the continuous curve in Fig. 8 is a plot of this equation). From eqn. (4), then, the estimate of $[Ca^{2+}]$ from aequorin luminescence may be expressed as:

$$[Ca^{2+}]\,(\mu M) = (1/(A \times L_{max})^{1/2{\cdot}37}) \times L^{1/2{\cdot}37}. \quad (5)$$

It follows from the equation that the use of an inappropriate calibration curve is equivalent to using an incorrect value for the constant A in eqn. (5). Therefore, even if an inappropriate calibration curve were used (or if there is an error in the estimate

of L_{max}), the estimate of $[Ca^{2+}]$ derived from luminescence is still *proportional to* the true spatial average $[Ca^{2+}]$.

Linearity of the relationship between the strength of contraction and peak estimated $[Ca^{2+}]$

From the discussion above, we conclude that $[Ca^{2+}]$ derived from aequorin luminescence should be proportional to, if not equal to, spatial average $[Ca^{2+}]$. Hence, the linearity of the relation between the strength of contraction and peak $[Ca^{2+}]$ should be genuine; only the exact-slope and intercept values of the relation might be subject to error.

This result may appear surprising at first because of the marked non-linearity of the steady-state $[Ca^{2+}]$–tension relation observed in skinned fibres (e.g. Hibberd & Jewell, 1982). However, the appreciable delay of tension development with respect to the $[Ca^{2+}]$ transient observed here and previously (Allen & Kurihara, 1980; Wier, 1980) indicate that $[Ca^{2+}]$ and force are far from steady state during the cardiac twitch. Hence, the linear relationship between F_{max} and peak $[Ca^{2+}]$, and between dF/dt_{max} and peak $[Ca^{2+}]$, characterizes the *transient* relation between tension and $[Ca^{2+}]$. Moreover, the linearity of the transient relation does not result from observing only a small section of a curvilinear steady-state relation; estimates of the steady-state $[Ca^{2+}]$–tension relation in intact muscles, obtained during tetanization, are markedly non-linear over the same range of $[Ca^{2+}]$ and tension, and fall to the left of the relations reported in this study (Yue, Marban & Wier, 1985*b*, 1986). Fabiato (1981, 1985*a*) reports that the relation between F_{max} and peak $[Ca^{2+}]$ in skinned heart cells superimpose upon the steady-state $[Ca^{2+}]$–tension relation, but his twitches are much slower in time course, and consequently may be nearer to steady state.

Interpretation of restitution and post-extrasystolic potentiation before and during exposure to ryanodine

Since the linearity of the relationship between the strength of contraction and peak $[Ca^{2+}]$ appears to be genuine, the results in Figs. 2 and 3 suggest that the restitution and post-extrasystolic potentiation of peak spatial average $[Ca^{2+}]$ should be described approximately by monoexponential functions, all with almost the same time constant as determined for the mechanical responses. It follows that there are, to the first degree of approximation, similar functions describing the restitution and post-extrasystolic potentiation of the *amount* of Ca^{2+} released from s.r. because most of the Ca^{2+} supplied to the myoplasm is believed to arise from Ca^{2+} released from s.r.

This later point bears some discussion. Estimates of the fraction of Ca^{2+} supplied to the myoplasm by s.r. range from 70% (Morad & Goldman, 1973) to ~ 100% (Fabiato, 1983; Marban & Wier, 1985). It might appear that these estimates are inconsistent with the results of Isenberg (1982), who found the magnitude of sarcolemmal Ca^{2+} currents to be substantially larger in isolated myocytes than previously expected from studies of multicellular preparations. It was therefore suggested that a rather large fraction of activator Ca^{2+} might derive from Ca^{2+} entry across the surface membrane (Fig. 8 of Isenberg (1982) shows ~ 25 μM increase in total Ca resulting from Ca current during 100 ms of depolarization in physiological perfusate). However, as noted in the same report, this suggestion did not consider the Ca^{2+} buffering of s.r., calmodulin, and other intracellular buffers. When these are

taken into account, it is less likely that Ca^{2+} entry, although larger than previously expected, could provide for a substantial fraction of activator Ca^{2+} (Fabiato, 1983).

Returning to our initial thought, we raise the question: how can the s.r. give rise to monoexponential functions describing the restitution and potentiation of the amount of Ca^{2+} released? One possible answer has been presented in detail (Yue *et al.* 1985*a*). Here we review that discussion in a more general form, and extend it to interpret the effects of ryanodine on restitution and p.e.s.p. curves.

I. Interpretation of physiological restitution and p.e.s.p. curves

Restitution has been proposed to arise from two assumed properties of the s.r.: (a) much of the Ca^{2+} sequestered by s.r. on a given beat is accumulated during the $[Ca^{2+}]$ transient, and (b) sequestered Ca^{2+} is only gradually made available for release in the interim between beats (Wood, Heppner & Weidmann, 1969; Gibbons & Fozzard, 1971; Tritthart, Kaufmann, Volkmer, Bayer & Krause, 1973; Morad & Goldman, 1973; Edman & Johannsson, 1976; Wohlfart, 1979; Yue *et al.* 1985*a*). Most of the evidence for these is inferential, but Fabiato (1985*b*) has recently presented some direct evidence favouring property a ('rapid phase' of Ca^{2+} accumulation) and property b.

Given these postulates, the time course of the restitution curve for the amount of Ca^{2+} released is determined by property b, and the plateau of the restitution curve is determined by the amount of Ca^{2+} accumulated during the preceding $[Ca^{2+}]$ transient plus the amount of Ca^{2+} that remained in the s.r. during the preceding Ca^{2+} release.

These ideas can be formalized by two models, both of which are functionally equivalent (Fig. 9*A*, left and right). The first of these (left) supposes that the s.r. is composed of two compartments, an uptake and a release compartment (U and R, respectively). Ca^{2+} is sequestered into the U store from Ca^{2+} released internally (Fig. 9*A*, 1; Morad & Goldman 1973) and from Ca^{2+} entering the cell across the surface membrane (Fig. 9*A*, 2; Fabiato 1985*c*). Ca^{2+} sequestered in the U store is not available for release; only gradually in the interim following a given $[Ca^{2+}]$ transient is Ca^{2+} translocated from U to R compartments (Fig. 9*A*, 3). Upon stimulation, all of the Ca^{2+} in the R store is released to myoplasm; the Ca in the U store at the time of the stimulus remains to contribute potentially to the following contraction.

Alternatively, the s.r. could be represented as a single compartment, with a channel for Ca^{2+} release that shows time-dependent recovery from inactivation (Fig. 9*A*, right). One example of this might be to suppose that after a given $[Ca^{2+}]$ transient, all the channels are in closed state C_a. With time, channels undergo a transition from closed state C_a to closed state C_b, according to the rate constant labelled 3. Upon stimulation, all channels in state C_b open (but not in C_a), allowing Ca^{2+} to be released. All other Ca^{2+} fluxes in this model are equivalent to those in the model at the left.

The monoexponential time course of restitution implies that either the translocation of Ca^{2+} from U to R compartments or the transition of channels from states C_a to C_b proceed according to first-order kinetics. The channel model interpretation would require the additional assumption that the amount of Ca^{2+} released is always proportional to the fraction of channels in state C_b just prior to stimulation.

The same models predict that the p.e.s.p. curve should also follow a monoexponential

time course, with a time constant identical to that of the restitution curve. During a very premature extrasystole, very little of the Ca^{2+} sequestered on the preceding steady-state beat can be released. Still, additional loading of the s.r. by transmembrane entry of Ca^{2+} (Fig. 9*A*, 2) does occur on the extrasystole. Then, on the subsequent, fully restituted post-extrasystole, all of the Ca^{2+} that was sequestered during two beats is released. Thus, we observe post-extrasystolic potentiation. As the prematurity

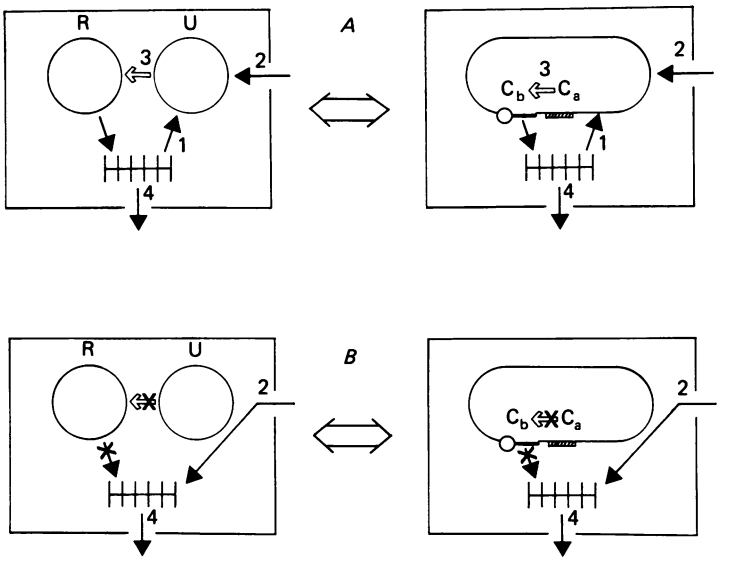

Fig. 9. Hypothesized excitation–contraction coupling events in heart cells. *A* corresponds to the physiological case. Ca^{2+} sequestered by s.r. can only gradually be made available for release in the interim between beats. This can be represented by a two-compartment model of s.r. (left: uptake, U; release, R), or by a one-compartment model of s.r. with Ca^{2+} channels exhibiting time-dependent recovery from inactivation (right: transition from closed states C_a to C_b). The myofilaments are represented by the hatched lines. *B* represents the case during exposure to ryanodine. The block of the release of Ca^{2+} from s.r. is represented by potential inhibition of either or both of the processes indicated by ×.

of an extrasystole is decreased, an increasing amount of Ca^{2+} is released during the extrasystole, and partially lost to the ensuing post-extrasystole (Fig. 9*A*, 4); the degree of potentiation is diminished. The decline of potentiation of fully restituted post-extrasystoles would therefore parallel the time course with which Ca^{2+} is made available for release for the extrasystole; the p.e.s.p. curve should follow a declining monoexponential time course, with time constant the same as for the restitution curve.

II. Interpretation of restitution and p.e.s.p. curves during exposure to ryanodine

If ryanodine inhibits the release of Ca^{2+} from s.r. (Fig. 9*B*, represented by inhibition of either or both processes labelled ×), then activator Ca^{2+} must be derived from Ca^{2+} entry across the surface membrane (Fig. 9*B*, 2). Moreover, if the s.r. cannot release Ca^{2+}, it must be saturated with sequestered Ca^{2+} (as might be inferred from Marban & Wier, 1985), and would therefore be unable to take up much Ca^{2+} in the steady state.

The former point might appear inconsistent with our original point that Ca^{2+} entry across surface membrane is insufficient to account for a substantial fraction of the Ca supplied to the myoplasm under physiological conditions, especially when confronted with our result that peak estimated $[Ca^{2+}]$ measured during exposure to ryanodine can be approximately the same as observed during physiological contractions (Figs. 1 and 4). The crucial concept to resolving this apparent conflict is this: if the s.r. is saturated, and therefore no longer sequesters Ca^{2+}, a substantial buffer of Ca^{2+} is removed; thus, a comparable amount of total Ca entry would be much more effective at raising free $[Ca^{2+}]$. Another factor that would enhance the increase in free $[Ca^{2+}]$ resulting from Ca^{2+} entry across the surface membrane is that Ca current is probably prolonged by ryanodine: the plateau duration of action potentials (at 30 % repolarization) in ferret papillary muscles increases from 150 to 400 ms in 5 μM-ryanodine (Wier, Yue & Marban, 1985), and Ca^{2+} currents are prolonged by ryanodine in rat ventricular cells (Mitchell, Powell, Terrar & Twist, 1984).

Then, in the presence of ryanodine, the restitution of activator Ca^{2+} might therefore be determined by the recovery of Ca current which has been determined to be very fast (fast time constant $\sim$ 50 ms in Kass & Sanguinetti, 1984), consistent with the restitution curve we determined for L/L_{max} in the presence of ryanodine. Furthermore, the strength of post-extrasystoles would reflect the magnitude of the sarcolemmal Ca current during post-extrasystoles. Given sufficient time to recover fully from inactivation (as should be the case with the p.e.s.i. = 3000 ms), Ca^{2+} conductance should not be a function of the e.s.i.; hence the p.e.s.p. curve should be flat, as we observed.

APPENDIX

Ca^{2+} is assumed to bind to troponin and calmodulin sites without co-operativity, so that Ca^{2+} binding to a given site B is described by:

$$\frac{d[B\text{–}Ca]}{dt} = k_{on}[Ca^{2+}]\{[B]_{tot} - [B\text{–}Ca]\} - k_{off}[B\text{–}Ca], \quad (A\ 1)$$

where the specific values for k_{on} and k_{off}, and the total concentrations of the buffers ($[B]_{tot}$) are listed in Table 3. The Ca^{2+} buffers were assumed to be at equilibrium with resting $[Ca^{2+}]$ prior to the release of Ca^{2+} from j.s.r.

The surface flux of Ca^{2+} release from j.s.r. (Fig. 6, CR) was described in the text, eqn. (2).

The surface flux of Ca^{2+} sequestration into f.s.r. (Fig. 6, CS) is assumed to be of the form:

$$CS = \frac{V_{max} \times [Ca^{2+}]}{K_m + [Ca^{2+}]}, \quad (A\ 2)$$

where V_{max} is $2{\cdot}232 \times 10^{-1}$ μmol s^{-1} m^{-2}, $K_m = 0{\cdot}25$ μM, and the surface area at the f.s.r.–m.f.s. interface is $2{\cdot}513 \times 10^{-12}$ m^2. These were selected to produce a realistic time course of relaxation. When the value for K_m obtained from studies of isolated s.r. vesicles was used (4·7 μM (Shigekawa, Finegan & Katz, 1976)), we were unable to obtain a satisfactory time course of relaxation despite adjustment of V_{max} over a wide range. A constant leakage flux of Ca^{2+} from f.s.r. ($= 6{\cdot}377 \times 10^{-2}$ μmol s^{-1} m^{-2};

Fig. 6, *l*) is assumed so that the level of resting [Ca^{2+}] is 0·1 μM in the absence of Ca^{2+} release.

Because of the circumferential symmetry of the cylindrical model, the angular coordinate can be ignored, and diffusion can be described according to the equation:

$$\frac{d[Ca^{2+}]}{dt} = D\left\{\frac{1}{r}\times\frac{\delta}{\delta r}\left(r\frac{\delta[Ca^{2+}]}{\delta r}\right)+\frac{\delta^2[Ca^{2+}]}{\delta z^2}\right\}-F([Ca^{2+}],t), \quad \text{(A 3)}$$

where r is the radial and z is the longitudinal coordinate of the cylinder (Crank, 1975); and F is the net non-diffusional flux resulting from Ca^{2+} buffer binding (eqn. (A 1)) and (if the equation is written for the interface of s.r. and m.f.s.) j.s.r. release (eqn. (2)), f.s.r. sequestration (eqn. (A 2)) or f.s.r. leakage. To obtain a numerical solution to the model, the half-sarcomere was divided into thirty elements, six elements radially and five elements longitudinally. The longitudinal dimension $SL/5$ of all elements was the same, as was the case for the radial dimension $R/6$ of all elements. Each element was addressed by the subscripts i,j, where i represented the radial address ($i = 1,2,\ldots,6$; 1 at the centre of the myofibril), and j represented the longitudinal address ($j = 1,2,\ldots,5$; 1 adjacent to the z-line). Given this geometry, the finite difference approximation corresponding to eqn. (A 3) is given by (Crank, 1975; eqns. (8·33) and (8·34)): for $i > 1$:

$$\frac{dC(i,j)}{dt} = D_r\left\{\left(2+\frac{1}{i-1}\right)(C(i+1,j)-C(i,j))-\left(2-\frac{1}{i-1}\right)(C(i,j)-C(i-1,j))\right\}$$
$$+D_l\{C(i,j+1)-2C(i,j)+C(i,j-1)\}-F(C(i,j),t),$$

and for $i = 1$:

$$\frac{dC(i,j)}{dt} = D_{re}\{C(i+1,j)-C(i,j)\}$$
$$+D_l\{C(i,j+1)-2C(i,j)+C(i,j-1)\}-F(C(i,j),t), \quad \text{(A 4)}$$

where $C(i,j) = [Ca^{2+}]$ in the i,j element, $D_r = D\times(5{\cdot}5)^2/2/R^2$, $D_l = D\times 5^2/SL^2$, $D_{re} = 8\times D_r$, and F is the net non-diffusional flux resulting from Ca^{2+} buffer binding and (if the equation is written for the interface of s.r. and m.f.s.) s.r. release, sequestration or leakage in the i,j element. Because the half-sarcomere in question was assumed to be surrounded by identical half-sarcomeres, no Ca^{2+} flux was allowed across any of the half-sarcomere boundaries. The model was implemented in IBM VS FORTRAN. A numerical solution was obtained on an IBM 4341 computer, using the commercially available subroutine DGEAR to solve the stiff differential equations comprising the model (IMSL, Houston, Texas). Division of the half-sarcomere into more than thirty elements was not possible due to constraints of computing speed and cost. To test the model for accuracy, the rate constants of the buffers were suitably adjusted so that, given a simple set of initial conditions, the model solution could be compared with the analytical solutions for radial and longitudinal diffusion in a cylinder in the presence of linear, instantaneous buffering (Crank, 1975). This very stringent test of the model resulted in errors that were at most 10 %. The model would be expected to be far more accurate during calculation of the physiological transient.

Spatial standard deviations of $[Ca^{2+}]$ were defined as:

$$\text{S.D.} = \frac{1}{V_T}\iiint_P ([Ca^{2+}]-[Ca^{2+}]_{aver})^2\,dx\,dy\,dz, \quad \text{(A 5)}$$

where P and V_T were defined as in eqn. (3), and $[Ca^{2+}]_{aver}$ is spatial average $[Ca^{2+}]$.

D.T.Y. acknowledges the encouragement and inspiration of Dr Kiichi Sagawa and Dr Jochen Schaefer. The work was supported in part by funds contributed by the Maryland Affiliate of the American Heart Association, and by U.S. Public Health Service Grant HL29473-02. D.T.Y. was supported by Medical Scientist Training Program Grant 5T32GM070309007. W.G.W. was supported in part by an Established Investigatorship of the American Heart Association.

REFERENCES

ALLEN, D. G. & BLINKS, J. R. (1978). Calcium transients in aequorin-injected frog cardiac muscle. *Nature* **273**, 509–513.

ALLEN, D. G. & KURIHARA, S. (1980). Calcium transients in mammalian ventricular muscle. *European Heart Journal* **1**, suppl. A, 5–15.

BAKER, P. F., HODGKIN, A. L. & RIDGWAY, E. B. (1971). Depolarization and calcium entry in squid axons. *Journal of Physiology* **218**, 709–755.

BLINKS, J. R., MATTINGLY, P. H., JEWELL, B. R., VAN LEEUWEN, M., HARRER, G. C. & ALLEN, D. G. (1978). Practical aspects of the use of aequorin as a calcium indicator: assay, preparation, microinjections, and interpretation of signals. *Methods in Enzymology* **57**, 292–328.

BLINKS, J. R., WIER, W. G., HESS, P. & PRENDERGAST, F. G. (1982). Measurement of Ca^{2+} concentrations in living cells. *Progress in Biophysics and Molecular Biology* **40**, 1–114.

BRAVENY, P. & KRUTA, V. (1958). Dissociation de deux facteurs: Restitution et potentiation dans l'action de l'amplitude de la contraction du myocarde. *Archives internationales de physiologie et de biochimie* **66**, 633–652.

BURKHOFF, D., YUE, D. T., FRANZ, M. R., HUNTER, W. C. & SAGAWA, K. (1984). Mechanical restitution of isolated perfused canine left ventricles. *American Journal of Physiology* **246**, H8–16.

CANNELL, M. B. & ALLEN, D. G. (1984). Model of calcium movements during activation in the sarcomere of frog skeletal muscle. *Biophysical Journal* **45**, 913–925.

CHEUNG, W. Y. (1980). Calmodulin plays a pivotal role in cellular regulation. *Science* **207**, 19–27.

COHEN, S. M. & BURT, C. T. (1977). ^{31}P nuclear magnetic relaxation studies of phosphocreatine in intact muscle: determination of intracellular free magnesium. *Proceedings of the National Academy of Sciences of the U.S.A.* **74**, 4271–4275.

CRANK, J. (1975). *The Mathematics of Diffusion*, 2nd edn., London: Oxford University Press.

DAWSON, M. J., GADIAN, D. G. & WILKIE, D. R. (1978). Muscle fatigue investigation by phosphorous nuclear magnetic resonance. *Nature* **274**, 861–866.

DRAPER, N. R. & SMITH, H. (1981). *Applied Regression Analysis*, 2nd edn., pp. 94, 462–468, 472. New York: Wiley-Interscience.

EDMAN, K. A. P. & JOHANNSSON, M. (1976). The contractile state of rabbit papillary muscle in relation to stimulation frequency. *Journal of Physiology* **254**, 565–581.

FABIATO, A. (1981). Myoplasmic free calcium concentration reached during the twitch of an intact isolated cardiac cell and during calcium-induced release of calcium from the sarcoplasmic reticulum of a skinned cardiac cell from the adult rat or rabbit ventricle. *Journal of General Physiology* **78**, 457–497.

FABIATO, A. (1983). Calcium-induced release of calcium from cardiac sarcoplasmic reticulum. *American Journal of Physiology* **245**, C1–14.

FABIATO, A. (1985*a*). Rapid ionic modifications during the aequorin-detected calcium transient in a skinned canine cardiac Purkinje cell. *Journal of General Physiology* **85**, 189–246.

FABIATO, A. (1985*b*). Time and calcium dependence of activation and inactivation of calcium-induced release of calcium from sarcoplasmic reticulum of a skinned canine cardiac Purkinje cell. *Journal of General Physiology* **85**, 247–289.

FABIATO, A. (1985*c*). Simulated calcium current can both cause calcium loading in and trigger calcium release from the sarcoplasmic reticulum of a skinned canine cardiac Purkinje cell. *Journal of General Physiology* **85**, 291–320.

GIBBONS, W. R. & FOZZARD, H. A. (1971). Voltage dependence and time dependence of contraction in sheep cardiac Purkinje fibers. *Circulation Research* **28**, 446–460.

HIBBERD, M. G. & JEWELL, B. R. (1982). Calcium- and length-dependent force production in rat ventricular muscle. *Journal of Physiology* **329**, 527–540.

HOFFMAN, B. F., BINDLER, E. & SUCKLING, E. E. (1956). Postextrasystolic potentiation of contraction in cardiac muscle. *American Journal of Physiology* **185**, 95–102.

ISENBERG, G. (1982). Ca entry and contraction in isolated bovine ventricular myocytes. *Zeitschrift für naturforschung* **37C**, 502–512.

JOHNSON, E. A. (1979). Force–interval relationship of cardiac muscle. In *Handbook of Physiology, The Cardiovascular System*, vol. I, ed. GEIGER, S. R. & BERNE, R. M., pp. 475–492. Bethesda, MD: American Physiological Society.

KASS, R. S. & SANGUINETTI, M. C. (1984). Inactivation of calcium channel current in the calf cardiac Purkinje fiber. *Journal of General Physiology* **84**, 705–726.

MARBAN, E. & WIER, W. G. (1985). Ryanodine as a tool to determine the contributions of calcium entry and calcium release to the calcium transient and contraction of cardiac Purkinje fibers. *Circulation Research* **56**, 133–138.

MITCHELL, M. R., POWELL, T., TERRAR, D. A. & TWIST, V. W. (1984). Ryanodine prolongs Ca-currents while suppressing contraction in rat ventricular muscle cells. *British Journal of Pharmacology* **81**, 13–15.

MOORE, E. D. W. (1984). Effects of pre-equilibration with Mg^{2+} on the kinetics of the reaction of aequorin with Ca^{2+} (abstr.). *Journal of General Physiology* **84**, 11a.

MORAD, M. & GOLDMAN, Y. (1973). Excitation–contraction coupling in heart muscle: membrane control of development of tension. *Progress in Biophysics and Molecular Biology* **27**, 257–313.

NEERING, I. R. & WIER, W. G. (1980). Kinetics of aequorin luminescence after step changes in calcium concentration: significance for interpretation of intracellular aequorin signals (abstr.). *Federation Proceedings* **39**, 1806.

PAGE, E. (1978). Quantitative ultrastructural analysis in cardiac membrane physiology. *American Journal of Physiology* **235**, C147–158.

POLIMENI, P. I. (1974). Extracellular space and ionic distribution in rat ventricle. *American Journal of Physiology* **227**, 676–683.

ROBERTSON, S. P., JOHNSON, J. D. & POTTER, J. D. (1981). The time-course of Ca^{2+} exchange with calmodulin, troponin, parvalbumin, and myosin in response to transient increases in Ca^{2+}. *Biophysical Journal* **34**, 559–569.

SHIGEKAWA, M., FINEGAN, J. M. & KATZ, A. M. (1976). Calcium transport ATPase of canine cardiac sarcoplasmic reticulum. *Journal of Biological Chemistry* **251**, 6894–6900.

SOLARO, R. J., WISE, R. M., SHINER, J. S. & BRIGGS, N. F. (1974). Calcium requirements for cardiac myofibrillar activation. *Circulation Research* **34**, 525–530.

SOMMER, J. R. & JOHNSON, E. A. (1979). Ultrastructure of cardiac muscle. In *Handbook of Physiology, The Cardiovascular System*, vol. I, ed. GEIGER, S. R. & BERNE, R. M., pp. 113–186. Bethesda, MD: American Physiological Society.

SUTKO, J. L. & KENYON, J. L. (1983). Ryanodine modifications of cardiac muscle responses to potassium-free solutions: evidence for inhibition of sarcoplasmic reticulum release. *Journal of General Physiology* **82**, 385–404.

SUTKO, J. L., WILLERSON, J. T., TEMPLETON, G. H., JONES, L. R. & BESCH, H. R. (1979). Ryanodine: its alterations of cat papillary muscle contractile state and responsiveness to inotropic interventions and a suggested mechanism of action. *Journal of Pharmacology and Experimental Therapeutics* **209**, 37–47.

TRITTHART, H., KAUFMANN, R., VOLKMER, H. P., BAYER, R. & KRAUSE, H. (1973). Ca-movement controlling myocardial contractility. I. Voltage, current and time dependence of mechanical activity under voltage clamp conditions (cat papillary muscles and trabeculae). *Pflügers Archiv* **338**, 207–231.

WANG, J. H. (1953). Tracer diffusion in liquids. IV. Self-diffusion of calcium ion and chloride ion in aqueous calcium chloride solutions. *Journal of the American Chemical Society* **75**, 1769–1770.

WIER, W. G. (1980). Calcium transients during excitation–contraction coupling in mammalian heart: aequorin signals of canine Purkinje fibers. *Science* **207**, 1085–1087.

WIER, W. G. & HESS, P. (1984). Excitation–contraction coupling in cardiac Purkinje fibers: effects of cardiotonic steroids on the intracellular [Ca^{2+}] transient, membrane potential and contraction. *Journal of General Physiology* **83**, 395–416.

WIER, W. G., KORT, A. A., STERN, M. D., LAKATTA, E. G. & MARBAN, E. (1983). Cellular calcium fluctuations in mammalian heart: direct evidence from noise analysis of aequorin signals in Purkinje fibers. *Proceedings of the National Academy of Sciences of the U.S.A.* **80**, 7367–7371.

WIER, W. G., YUE, D. T. & MARBAN, E. (1985). Effects of ryanodine on intracellular Ca^{2+} transients in canine cardiac Purkinje fibers and ferret ventricular muscle. *Federation Proceedings* **44**, 2989–2993.

WOHLFART, B. (1979). Relationship between peak force, action potential duration and stimulus interval in rabbit myocardium. *Acta physiologica scandinavica* **106**, 395–409.

WOOD, E. H., HEPPNER, R. L. & WEIDMANN, S. (1969). Inotropic effects of electric currents. *Circulation Research* **24**, 409–445.

YUE, D. T., BURKHOFF, D., FRANZ, M. R., HUNTER, W. C. & SAGAWA, K. (1985*a*). Postextrasystolic potentiation of the isolated canine left ventricle: relationship to mechanical restitution. *Circulation Research* **56**, 340–350.

YUE, D. T., MARBAN, E. & WIER, W. G. (1985*b*). Relationship between force and intracellular [Ca^{2+}] in tetanized ventricular myocardium (abstr.). *Biophysical Journal* **47**, 353a.

YUE, D. T., MARBAN, E. & WIER, W. G. (1986). Relationship between force and intracellular [Ca^{2+}] in tetanized mammalian heart muscle. *Journal of General Physiology* **87**, 223–242.

YUE, D. T. & WIER, W. G. (1985). Estimation of intracellular [Ca^{2+}] by nonlinear indicators: a quantitative analysis. *Biophysical Journal* **48**, 533–537.

YUE, D. T., WIER, W. G. & SAGAWA, K. (1984). Direct measurement of the intracellular [Ca^{2+}] transients underlying the cardiac force–interval relationship (abstr.). *Sixth Proceedings of the Cardiovascular Systems Dynamics Society*, pp. 1–4. Philadelphia: University of Pennsylvania.

ZIEMER, R. E., TRANTER, W. H. & FANNIN, D. R. (1983). *Signals and systems: continuous and discrete*, pp. 373–376. New York: Macmillan.